Vegetable Research

ARTICLE

Open Access

https://doi.org/10.48130/vegres-0025-0011

Vegetable Research **2025**, 5: e013

Phenotypic characteristics and transcriptome of wax gourd embryonic root development under high auxin stress

Xiaoxin Cheng[1,2], Jiesheng Hong[1,2], Xuling Zhai[1,2], Baochen Wang[1,2], Renlian Mo[1,2], Dian Li[1,2], Wenrui Liu[1,2], Jinqiang Yan[1,2*] and Biao Jiang[1,2*]

[1] *Vegetable Research Institute, Guangdong Academy of Agricultural Sciences, Guangzhou 510640, China*
[2] *Guangdong Key Laboratory for New Technology Research of Vegetables, Guangzhou 510640, China*
* Corresponding authors, E-mail: yanjinqiang@gdaas.cn; jiangbiao@gdaas.cn

Abstract

Wax gourd is an important horticultural crop, and auxin plays a crucial role in its growth and development. However, excessive concentrations of auxin can inhibit plant growth. In this study, we investigated the phenotypic characteristics and conducted a transcriptomic analysis of wax gourd embryonic root development under high auxin concentration. Phenotypic observations revealed that as auxin concentration increased, the primary root of the wax gourd radicle became shorter, the number of lateral roots increased, and the length of lateral roots fluctuated. Transcriptomic analysis identified 1,305 differentially expressed genes (DEGs), including 43 genes associated with auxin, as determined by GO and KEGG annotations. We further focused on 10 key genes with significant differential expression and validated the results using qRT-PCR, which aligned with the transcriptomic date. Notably, the expression of *ABCB* increased with higher IAA concentrations, while *PILS7*, *LAX3*, *IAA16*, *FRQ1*, and *MYBS3* showed significant downregulation at 600 μM IAA. Conversely, *SAUR32* and *SAUR71* were significantly upregulated under the same conditions, while the expression of *PIN3* and *KRP1* exhibited variable patterns. These findings suggest that these genes are key regulators of wax gourd embryonic root responses to high auxin concentration. This study provides valuable insights into the molecular mechanism underlying auxin-induced stress in wax gourd and lays a foundation for further research on its response mechanisms.

Citation: Cheng X, Hong J, Zhai X, Wang B, Mo R, et al. 2025. Phenotypic characteristics and transcriptome of wax gourd embryonic root development under high auxin stress. *Vegetable Research* 5: e013 https://doi.org/10.48130/vegres-0025-0011

Introduction

As one of the oldest crops in the Cucurbitaceae family, wax gourd (*Benincasa hispida*, 2n = 2x = 24) is native to southern China, India, Thailand, and Myanmar. It is known for its high yield and excellent storage resistance[1]. Wax gourd fruit ranges in weight from a few kilograms to 20 kg, with some reaching up to 50 kg, making it an important vegetable crop in China[2]. Beyond its agricultural value, wax gourd possesses rich nutritional and medicinal properties. The fruit is rich in protein, carbohydrates, inorganic salts, vitamins, and other essential nutrients[3]. Additionally, the skin of wax gourd has been shown to aid in the prevention and treatment of metabolic diseases, such as hyperglycemia, obesity, and cardiovascular disease[4].

Auxin is a crucial regulator of plant growth and development, primarily influencing processes such as cell division and differentiation[5]. Additionally, auxin plays a central role in various physiological processes by mediating chemical signaling, enabling plants to respond to a wide range of biotic and abiotic stresses[6,7], including resistance to Rice dwarf virus (RDV)[8], heavy metal stress[9], and salt stress[10]. Indole-3-acetic acid (IAA) is the most prominent natural auxin in plants, existing in both free and conjugated forms[11]. A network of auxin-responsive genes detects and responds to auxin through complex signal transduction pathways, maintaining a delicate balance in plant growth and development. For instance, in nutrient-deficient soil, auxin rapidly accumulates in root hair cells, elevating levels of reactive oxygen species (ROS), and nitric oxide (NO), which promotes root hair growth as an adaptive response to environmental challenges[12]. Auxin synthesis is tightly regulated by both internal and external factors, and its concentration has a direct impact on plant growth and development. At low concentrations, auxin promotes growth, whereas high concentrations can inhibit it[13]. At low auxin levels, the transcriptional corepressor TPL suppresses auxin-regulated transcription by mediating the interaction between AUX/IAA proteins and ARFs (Auxin Response Factors). At high auxin levels, the SCF^{TIR1} complex binds to auxin, targeting AUX/IAA proteins for degradation via the ubiquitin-proteasome pathway[14]. These sophisticated regulatory mechanisms underscore the importance of auxin in plant development. A deeper understanding of auxin synthesis, signaling, and its interaction with specific genes is essential to unravelling the complexities of plant growth and response to environmental stimuli.

The root system is fundamental to plant growth and development, as it absorbs water and mineral nutrients from the soil. In response to changing environmental conditions, the root system adapts its architecture, regulates transcription factors, and modulates hormone levels to enhance plant fitness and survival[15–17]. Auxin plays a central role in shaping root system architecture[18]. Research has demonstrated that exogenous auxin promotes lateral root growth and alleviates the inhibitory effects of *ERF012* overexpression on root development[19]. Additionally, studies indicate that auxin signaling is mediated through specific modules, including *SLR/IAA14-ARF7*, *ARF19*, *BDL/IAA12-ARF5*, *TRH1*, and *PIN2*. These modules are crucial for driving root epidermal cell differentiation and the root gravitropic response[18,20,21]. Such findings highlight the intricate regulatory role of auxin in root system development and its potential for enhancing plant adaptation to environmental challenges.

NPA is an auxin transport inhibitor. In our preliminary experiments, we observed that the inhibitory effects of 600 to 1,000 μM IAA were similar to those of 1–5 μM NPA. Based on these findings, we selected the 600 to 1,000 μM IAA concentration gradient for

© The Author(s)

further in-depth investigation. In this study, we investigated the phenotypic characteristics and transcriptomic changes associated with wax gourd embryonic root development under high auxin stress. Our analysis identified differentially expressed genes and explored their roles in regulating root organ development in response to elevated auxin levels. These findings provide new insights into the molecular mechanisms underlying wax gourd embryonic root development under high auxin stress, contributing to a deeper understanding of its adaptive responses.

Materials and methods

Plant materials

The inbred line B227 of wax gourd (*B. hispida*) was provided by the Vegetable Research Institute, Guangdong Academy of Agricultural Sciences (Guangdong, China).

High auxin stress treatments

The seed coats were removed, and the seeds were soaked in warm water at 55 °C for 8 h. Afterward, the seeds were placed on filter paper moistened with different concentrations of IAA (600, 800, 1,000 μM) in culture dishes. The control seeds were moistened with distilled water. The seedlings were then cultivated at 32 °C in a greenhouse under darkness for 4 d until germination.

Root phenotype assessment

Four days after germination, the lengths of the primary roots and lateral roots were measured using a ruler with six biological replicates, and the number of lateral roots was recorded. Statistical analyses were subsequently performed using SPSS software.

RNA extraction, Illimina sequencing, and differentially expressed gene analyses

RNA extraction and Illumina sequencing were conducted by Metware Biotechnology Co., Ltd. (Wuhan, China), differential gene expression analysis and functional enrichment analysis were performed using the online tools available on the Majorbio Cloud Platform (www.majorbio.com). The processes for RNA extraction, Illumina sequencing, quality control, read mapping, and differential expression gene (DEG) enrichment analysis were as follows:

Total RNA was extracted using ethanol precipitation and the CTAB-PBIOZOL method. RNA purity, concentration, and integrity were assessed using a NanoPhotometer, Qubit 4.0, and Qsep400, respectively. High-quality RNA was reverse transcribed into cDNA and amplified by PCR to construct the transcriptome library. Paired-end sequencing of the RNA-seq libraries was conducted on the Illumina NovaSeq 6000 platform (Illumina, San Diego, CA, USA). Strict quality control was applied to the raw sequencing data using fastp[22] to ensure high-quality reads. An index was built using HISAT[23], and clean reads were aligned to the reference genome of wax gourd (wax gourd B227 v1 Genome[1]). Gene expression levels were quantified using FPKM (Fragments Per Kilobase of transcript per Million fragments mapped) with featureCounts. Graphpad Prism 9.5 was used to analyse and visualize Pearson correlation. Principal component analyses (PCA) were performed using FactoMineR R package and visualized with ggplot R package. Differential expression analysis between sample groups was conducted using DESeq2[24,25], with criteria set as $\log_2$FoldChange ≥ 1 and FDR ≤ 0.05. Functional enrichment analysis was performed using the Gene Ontology (GO) (www.geneontology.org) and Kyoto Encyclopedia of Genes and Genomes (KEGG) (www.genome.jp/kegg) databases.

Quantitative real-time RT-PCR

Total RNA was extracted from wax gourd embryonic roots grown under normal and high auxin conditions using the *TransZol* Up Plus RNA Kit. Extracted RNA was reverse-transcribed into cDNA using *TransScript*® All-in-One First-Strand cDNA Synthesis SuperMix for qPCR (with One-Step gDNA Removal). qRT-PCR was conducted using *UBIQUITIN* as the internal reference gene, with specific primers listed in Supplementary Table S1[26]. Each experiment included three biological replicates and three technical replicates. Relative gene expression levels were calculated using the $2^{-\Delta\Delta C_T}$ method. A heat map based on RNA-seq data was generated by Tbtools[27].

Results

Morphological characterization of wax gourd embryonic roots under high auxin

Wax gourd seeds were treated with 600, 800, and 1,000 μM IAA, with ddH_2O serving as the control. After 4 d of germination, the main root length and the number of lateral roots were recorded. The germination rate and morphological development of the seeds was illustrated in Supplementary Fig. S1; Fig. 1, respectively, and the quantitative analysis of root characteristics are presented in Fig. 2. The results revealed that the germination rates ranging from 62.5% to 78.7%. Seeds treated with ddH_2O had the longest main roots and the highest number of lateral roots. With increasing IAA concentrations, the main root length decreased, and the number of lateral roots declined, showing statistically significant differences ($p < 0.05$) among treatments. Interestingly, seeds treated with 800 μM IAA exhibited the highest number of lateral roots, followed by the ddH_2O control, while those treated with 1,000 μM IAA had the fewest lateral roots.

RNA-seq, quality assessment, and differentially expressed gene (DEGs) analyses

The embryonic roots treated with 0 μM IAA and 1,000 μM IAA were examined by RNA-seq, each with three biological replicates. After filtering low-quality reads, 41,593,638 to 46,908,870 clean reads were obtained. The error rate of all samples was controlled at approximately 0.03%. The Q20 and Q30 values were greater than 90%, and the GC content ranged from 42.65% to 43.88%. No GC or AT bias was observed in any sample.

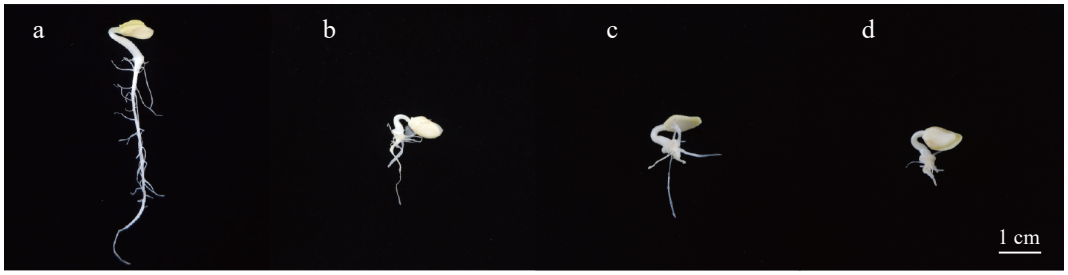

Fig. 1 Phenotype of wax gourd seedlings treated with different concentrations of IAA. (a) Control, (b) treatment with 600 μM IAA, (c) treatment with 800 μM IAA, (d) treatment with 1,000 μM IAA. Scale bar = 1cm.

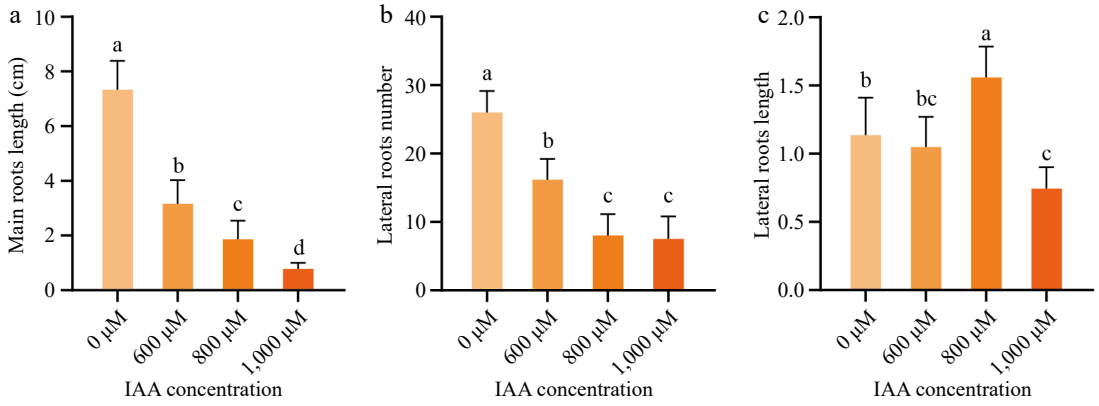

Fig. 2 Morphological changes during early roots development in different concentrations of IAA. (a) Main root length, (b) lateral root length, and (c) the number of lateral roots of wax gourd seed embryonic treated with 0, 600, 800, and 1,000 μM IAA. Data are presented as mean ± standard error (n = 6). Different lowercase letters on the bars indicate significant differences at $p < 0.05$ (Duncan's multiple range test).

Pearson correlation and PCA were performed to assess the quality of the transcriptomic data (Fig. 3a, b). High correlation coefficients among replicates demonstrated the consistency of transcriptional changes within each sample. PC1 accounted for 48.1% of the variance, while PC2 explained 21.8%. Samples within the same group were tightly clustered, while those from different groups were well separated. These results indicate that the sequencing quality was sufficient for subsequent analyses.

A total of 1,305 DEGs were identified, of which 575 were upregulated, and 730 were downregulated (Fig. 3). Among the most significantly affected genes (top 50 DEGs, ranked by $\log_2$FoldChange), many were involved in redox-related processes. These included genes encoding proteins such as PF00067.25 (Cytochrome P450), PF00155.24 (Aminotransferase class I and II), and PF02373.25 (JmjC domain, hydroxylase). Additionally, several genes related to regulating gene expression, such as transcription factors, were identified

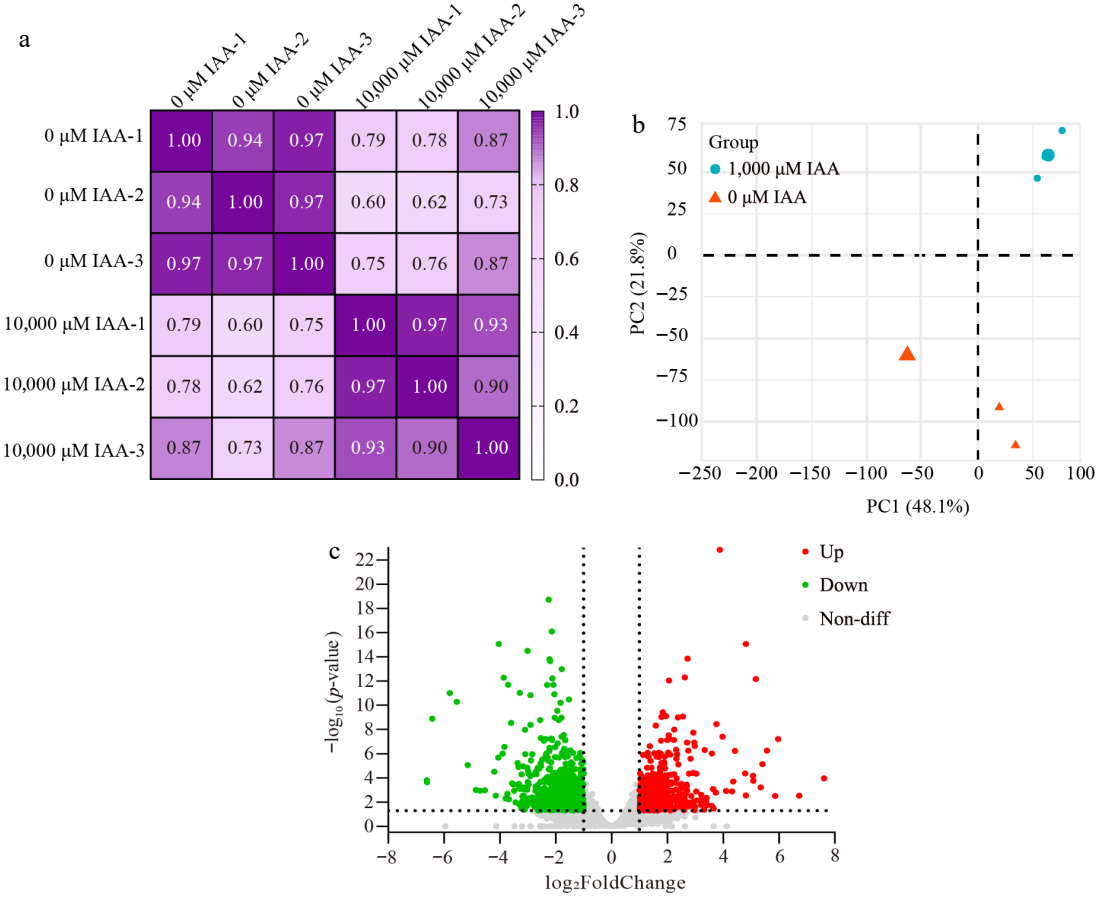

Fig. 3 Pearson correlation, PCA analysis, and Volcano plot of differentially expressed genes. (a) Correlation matrix and cluster dendrogram of the whole dataset. The analysis compared the transcriptomes of all samples with three biological replicates. Dark purple indicates strong correlations, while light purple indicates weaker correlations. (b) PCA of samples grouped by treatment. Blue dots represent 1,000 μM IAA-treated samples, and orange triangles represent 0 μM IAA-treated samples. (c) Volcano plot showing DEGs between the two treatment groups. The x-axis represents the $\log_2$FoldChange of gene expression levels, while the y-axis represents the significance of the DEGs. Red dots indicate upregulated genes, green dots indicate downregulated genes, and gray dots indicate non-differentially expressed genes.

among the top 50 DEGs, including PF00847.23 (AP2 domain), PF03106.18 (WRKY DNA-binding domain), and PF00010.29 (Helix-loop-helix DNA-binding domain). Other functional classifications among the top 50 DEGs included phosphorylation and dephosphorylation during signal transduction, hydrolysis reactions, such as glycosidases and proteases, those involved in transferring groups, such as glycosyltransferases and maintaining cell structure, and cytoskeleton. Notably, the largest proportions of these DEGs belonged to the Protein kinase domain (22 members), Cytochrome P450 (21 members), AP2 domain (17 members), and Leucine-rich repeat (10 members).

Function and pathway enrichment analyses

We performed the GO and KEGG enrichment analysis according to the 1,305 DEGs to annotate their functions in responding to high auxin. A total of 2,353 Gene Ontology (GO) terms were included in the GO enrichment analysis. The results revealed that 1,616 terms were associated with biological processes, 529 with molecular functions, and 208 with cellular components. The three most significantly enriched terms were heme binding (GO:0020037), response to auxin (GO:0009733), and oxidoreductase activity, acting on paired donors, with incorporation or reduction of molecular oxygen (GO:0016705), all of which are closely related to auxin response or potential interplay with auxin signaling[28,29].

To further explore functional enrichment, we analyzed 31 terms with the highest degree of enrichment among the DEGs (Fig. 4). Regarding biological processes, the majority of genes were enriched in cellular processes, with 320 upregulated and 341 downregulated genes. Other enriched categories included metabolic processes, response to stimuli, and biological regulation. For cellular components, most genes were associated with cellular anatomical entities and protein-containing complexes. In terms of molecular function, DEGs were primarily involved in binding, catalytic activity, and transcription regulator activity.

A total of 108 pathways were analyzed using KEGG, with the 20 most significantly enriched pathways shown in Fig. 5. The top five pathways were biosynthesis of secondary metabolites, phenylpropanoid biosynthesis, plant-pathogen interaction, plant hormone signal transduction, and nitrogen metabolism, involving 136, 28, 55, 57, and eight genes, respectively. Furthermore, we analyzed DEGs involved in the Plant hormone signal transduction pathway (ko04075) and classified them into five functional groups: auxin-related, brassinosteroid-related, signaling-related, transcription factors, and others. This classification aimed to investigate the cross-talk network between auxin and other plant hormones and factors. The results showed 13, 14, 10, 13, and seven genes in each category, respectively. Notably, most genes encoding auxin-responsive proteins, such as *SAUR* and *IAA*, were downregulated, whereas others, including indole-3-acetic acid-amido synthetase gene *GH3*, were upregulated (Supplementary Table S2).

Transcriptome validation by RT-qPCR

To validate the accuracy of the RNA-seq results, 10 genes with significant expression differences (eight up-regulated genes and two down-regulated genes, Supplementary Table S3) were selected for qRT-PCR analysis. Furthermore, we conducted qPCR analysis for 600 and 800 μM IAA treatments to enrich the data and further understand the effects of different IAA concentrations. The results of RT-qPCR showed a high degree of consistency with the RNA-seq data (Fig. 6), confirming the reliability of the transcriptomic analysis. Among the selected genes, the expression of *ABCB19* increased progressively with higher concentrations of IAA, indicating its potential role in IAA transport and regulation. Conversely, the expression levels of *PILS7*, *LAX3*, *IAA16*, *FRQ1*, and *MYBS3* were significantly downregulated under treatment with 600 μM IAA. In contrast, *SAUR32* and *SAUR71* were significantly upregulated under the same conditions. Interestingly, the expression of *PIN3* and *KRP1* showed variable trends across treatments, reflecting possible complex or condition-specific regulatory mechanisms that warrant further investigation.

Discussion

In this study, we examined the phenotypic characteristics of wax gourd embryonic roots germinating under high concentrations of IAA. As the concentration increased, the main roots exhibited a reduction in length, and the lateral roots showed a decline in number. This observation aligns with previous studies, which have demonstrated that exogenous IAA application inhibits root growth by reducing cell size rather than by inhibiting cell production rates[30–32]. For instance, in *Arabidopsis thaliana*, excessive auxin accumulation in the root meristem leads to increased expression of

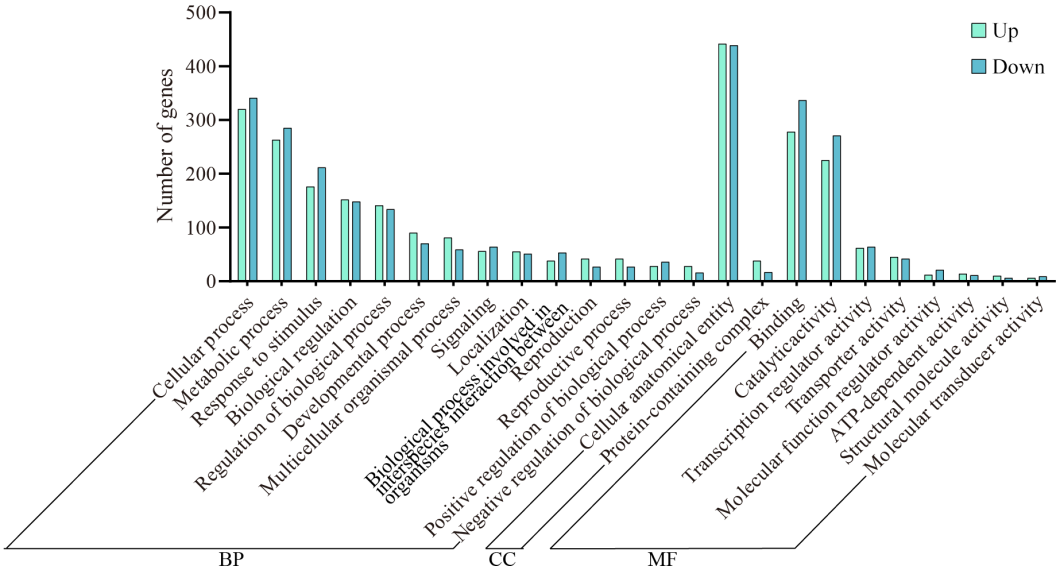

Fig. 4 Enrichment analysis of GO differentially expressed gene in wax gourd embryonic roots. BP represents biological process, CC represents cellular component, and MF represents molecular function.

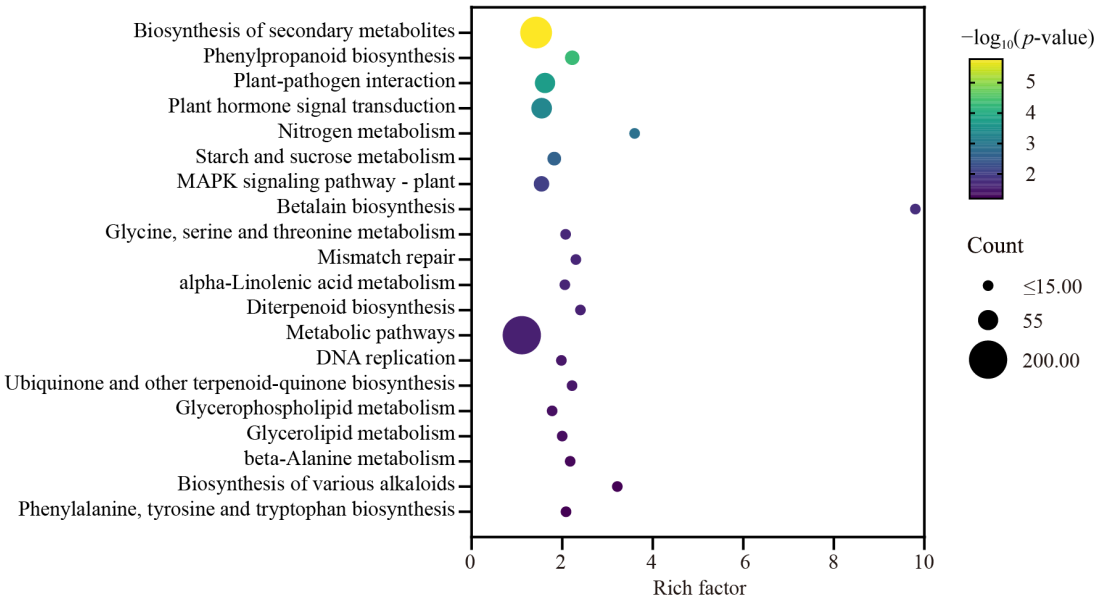

Fig. 5 KEGG enrichment analysis of differentially expressed gene in wax gourd embryonic roots. The X-axis represents the enrichment factor of different KEGG pathways and the Y-axis represents different KEGG pathways. Dot colors indicate different p values, while dot sizes represent the number of genes associated with each pathway.

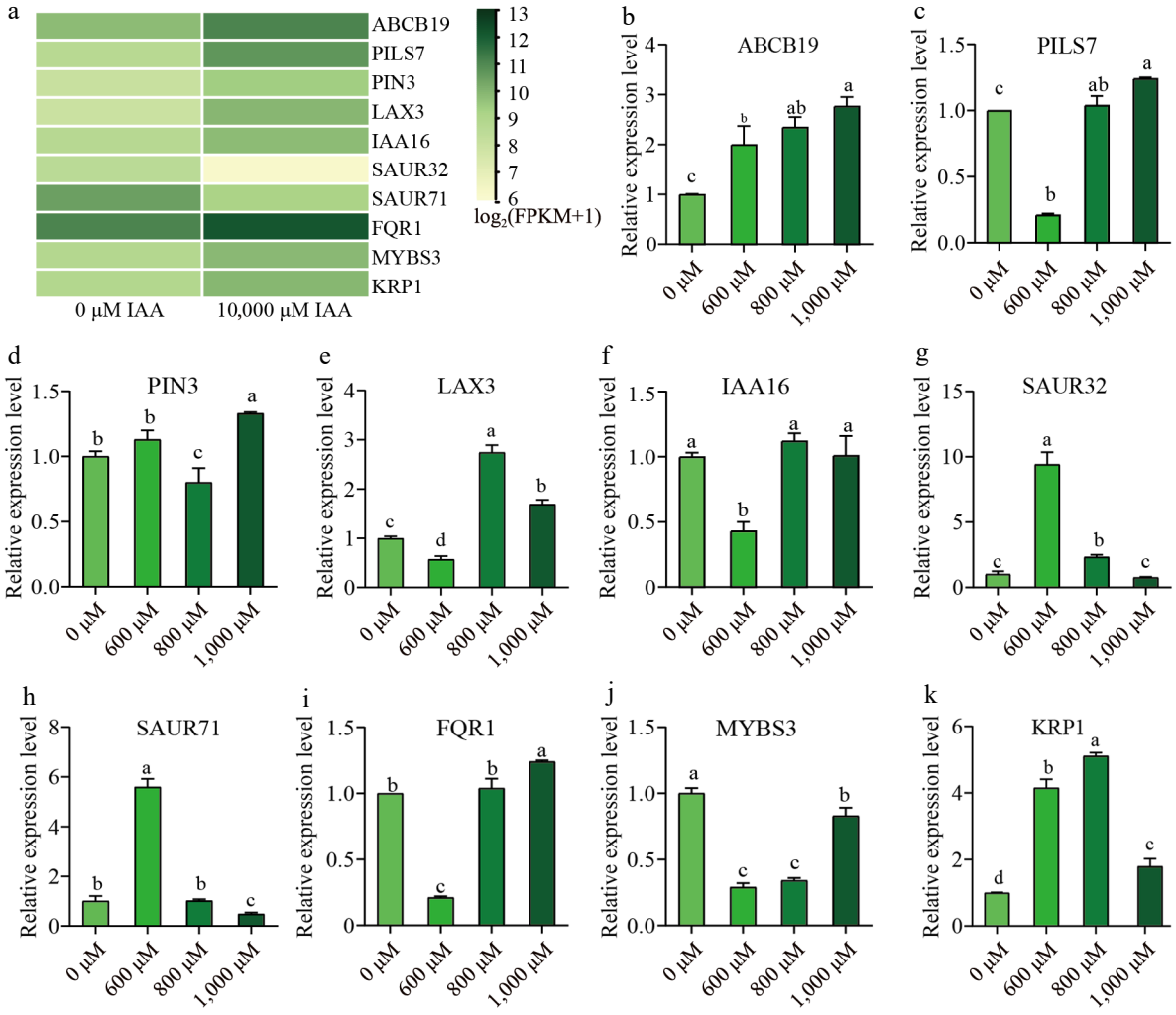

Fig. 6 Validation of RNA-Seq data using qRT-PCR analysis. (a) Heat map of 10 selected DEGs based on RNA-seq data. (b)–(k) Expression pattern validation analysis by qRT-PCR after 600, 800, and 1,000 μM IAA treatment. X-axis indicates treatment with different IAA concentrations, Y-axis indicates gene relatively exprssion level. Expression levels were represented as mean ± SE. Error bars indicate the standard error calculated from three replicates. Different lowercase letters above the bars indicate significant differences ($p < 0.05$, Duncan's multiple range test).

PIN1 and *PIN4*, and decreased expression of *PIN2* and *AUX1*. This redistribution facilitates auxin transport to the root elongation zone, thereby inhibiting root elongation[33]. Based on these findings, we speculate that the observed reduction in main root length in wax gourd may result from the inhibitory effect of IAA on root cell elongation.

To identify specific genes responding to high auxin stress in wax gourd roots, we selected various auxin signaling-related genes from the transcriptomic data and validated their expression using qRT-PCR. The results indicate that these genes play crucial roles in maintaining auxin homeostasis. Auxin efflux transporters such as *PIN*, *ABCB,* and *PILS7*, are essential for root growth and the development of root architecture[34,35]. A study demonstrated that knock-down and genome editing of this genetically linked group of ABCB transporters led to a significant reduction in auxin oscillation and lateral root densities[36]. *ABCB* transporters, which are typically apolarly localized, actively transport auxin against its concentration gradient in an energy-dependent manner[37]. In this study, *ABCB* expression was found to increase with higher IAA concentrations, suggesting its role in facilitating auxin efflux under high auxin conditions. In terms of auxin influx carriers, *LAX3* expression peaked under 800 μM IAA treatment, followed by 1,000, 600, and 0 μM. This trend closely mirrored the changes in lateral root length. Previous studies have shown that changes in the expression of auxin influx carriers like *LAX3* can influence lateral root development by enhancing growth parameters[38,39]. Otherwise, auxin produced in the lateral root would be transported to other issues to trigger cell separation by inducing the expression of *LAX3* and *PIN* transporters[40]. Auxin-responsive proteins also exhibited significant changes in expression under high IAA concentrations. Notably, *IAA16*, *SAUR32,* and *SAUR71* showed differential expression under 600 μM IAA treatment. Zhu et al. reported that *ArAux/IAA16* was significantly differentially expressed after 300 mg/L IAA treatment in *Acer rubrum*. And overexpression of *ArAux/IAA16* in transgenic plants inhibited adventitious root development[41]. Although research on *SAUR32* and *SAUR71* in root development is limited, Wang et al. found that IAA treatment altered root development in *Salvia miltiorrhiza* seedlings, with *SmSAUR* family genes influencing root parameters[42]. These findings are consistent with our results, suggesting that *SAUR32* and *SAUR 71* play roles in auxin-mediated root development.

Additionally, we identified two stress-related genes, *FQR1* and *MYBS3*, whose expression levels increased with IAA concentration regardless of CK. Previous studies have shown that *FQR1* mitigates oxidative damage and enhances photosynthetic capacity under high-temperature stress[43]. Similarly, *MYBS3* is highly expressed in cotyledonary embryos induced by high IAA concentrations and 2,4-D in immature male flowers[44]. Another notable gene identified was *KRP1*, which encodes a calcium-binding protein involved in inhibiting cell proliferation and enlargement during grain filling and seed germination in rice[45]. The varied expression of KRP1 observed in this study suggests its potential role in regulating root architecture under high auxin conditions.

The observed reduction in main root length, coupled with the variable lengths and numbers of lateral roots, underscores the complex role of auxin in shaping root architecture. These findings enhance our understanding of plant hormone interactions and have potential implications in improving root development in horticultural crops under stress conditions. However, this study raises new questions about the precise mechanisms by which these genes interact to regulate root architecture under high auxin stress. Future research should focus on elucidating the interaction networks of these key genes, possibly through gene knockout or overexpression studies. Additionally, exploring their interactions with other hormones and environmental factors will provide a more comprehensive understanding of root development in wax gourd and other corps.

Conclusions

In conclusion, this study highlights the significant impact of high auxin concentrations on the growth and development of wax gourd embryonic roots. The phenotypic analysis demonstrated that elevated auxin levels inhibited primary root elongation while promoting lateral root formation with fluctuating lengths. Transcriptomic analysis identified key auxin-related genes, revealing distinct expression patterns under high auxin stress. Notably, the expression of *ABCB* increased with higher IAA concentrations, while *PILS7*, *LAX3*, *IAA16*, *FRQ1*, and *MYBS3* showed significant downregulation at 600 μM IAA. Conversely, *SAUR32* and *SAUR71* were significantly upregulated under the same conditions, while the expression of *PIN3* and *KRP1* exhibited variable patterns, emphasizing their roles in auxin response regulation. These findings enhance our understanding of the molecular mechanisms of auxin-induced stress in wax gourd and provide a foundation for further exploration of adaptive strategies to optimize wax gourd growth under varying auxin conditions.

Author contributions

The authors confirm contribution to the paper as follows: study conception and design: Jiang B, Yan J, Liu W, Cheng X; data collection: Cheng X; analysis and interpretation of results: Yan J, Zhai X, Cheng X; draft manuscript preparation: Cheng X; review and editing: Jiang B, Cheng X; experiment performing: Hong J, Wang B, Mo R, Li D, Cheng X. All authors reviewed the results and approved the final version of the manuscript.

Data availability

Wax gourd genome: http://cucurbitgenomics.org/organism/22. The sequencing data: https://trace.ncbi.nlm.nih.gov/Traces/?view=study&acc=SRP570091

Acknowledgments

This work was supported by 2024 Guangdong Rural Revitalization Strategy Special Project (2024-NPY-00-024, 2024-440400-103010206-0002), the Science and Technology Program of Guangdong (2023A0505090005, 2024A1515012539), and the Training Plan for Young and Middle-Aged Discipline Leaders of GDAAS (R2023PY-JX007).

Conflict of interest

The authors declare that they have no conflict of interest.

Supplementary information accompanies this paper at (https://www.maxapress.com/article/doi/10.48130/vegres-0025-0011)

Dates

Received 6 December 2024; Revised 24 January 2025; Accepted 14 February 2025; Published online 16 April 2025

References

1. Xie D, Xu Y, Wang J, Liu W, Zhou Q, et al. 2019. The wax gourd genomes offer insights into the genetic diversity and ancestral cucurbit karyotype. *Nature Communications* 10:5158

2. The Institute of Vegetables and Flowers Chinese Academy of Agricultural Sciences. 2010. *Chinese vegetable cultivation*. China: China Agriculture Press. pp. 557–58
3. Sreenivas KM, Chaudhari K, Lele SS. 2011. Ash gourd peel wax: extraction, characterization, and application as an edible coat for fruits. *Food Science and Biotechnology* 20:383–87
4. Gu M, Fan S, Liu G, Guo L, Ding X, et al. 2013. Extract of wax gourd peel prevents high-fat diet-induced hyperlipidemia in C57BL/6 Mice via the inhibition of the PPARγ pathway. *Evidence-Based Complementary and Alternative Medicine* 2013:342561
5. Perrot-Rechenmann C. 2010. Cellular responses to auxin: division versus expansion. *Cold Spring Harbor Perspectives in Biology* 2:a001446
6. Wawrzyńska A, Sirko A. 2024. Sulfate availability and hormonal signaling in the coordination of plant growth and development. *International Journal of Molecular Sciences* 25:3978
7. Choi HW. 2024. From the photosynthesis to hormone biosynthesis in p lants. *The Plant Pathology Journal* 40:99–105
8. Qin Q, Li G, Jin L, Huang Y, Wang Y, et al. 2020. Auxin response factors (ARFs) differentially regulate rice antiviral immune response against rice dwarf virus. *PLoS Pathogens* 16:e1009118
9. Zhang Y, Yang C, Liu S, Xie Z, Chang H, et al. 2024. Phytohormones-mediated strategies for mitigation of heavy metals toxicity in plants focused on sustainable production. *Plant Cell Reports* 43:99
10. Zheng L, Hu Y, Yang T, Wang Z, Wang D, et al. 2024. A root cap-localized NAC transcription factor controls root halotropic response to salt stress in Arabidopsis. *Nature Communications* 15:2061
11. Zhao Y. 2014. Auxin biosynthesis. *The Arabidopsis Book* 2014:e0173
12. Gabarain VB, Ibeas MA, Salinas-Grenet H, Estevez JM. 2024. Auxin signaling gets oxidative to promote root hair growth. *Molecular Plant* 17:696–98
13. Zhang Q, Gong M, Xu X, Li H, Deng W. 2022. Roles of auxin in the growth, development, and stress tolerance of horticultural plants. *Cells* 11:2761
14. Saini S, Sharma I, Kaur N, Pati PK. 2013. Auxin: a master regulator in plant root development. *Plant Cell Reports* 32:741–57
15. Rogers ED, Benfey PN. 2015. Regulation of plant root system architecture: implications for crop advancement. *Current Opinion in Biotechnology* 32:93–98
16. Grunewald W, De Smet I, Lewis DR, Löfke C, Jansen L, et al. 2012. Transcription factor WRKY23 assists auxin distribution patterns during Arabidopsis root development through local control on flavonol biosynthesis. *Proceedings of the National Academy of Sciences of the United States of America* 109:1554–59
17. Rellan-Alvarez R, Lobet G, Dinneny JR. 2016. Environmental Control of Root System Biology. *Annual Review of Plant Biology* 67:619–42
18. Cavallari N, Artner C, Benkova E. 2021. Auxin-regulated lateral root organogenesis. *Cold Spring Harbor Perspectives in Biology* 13:a039941
19. Huang Y, Liu L, Hu H, Tang N, Shi L, et al. 2022. *Arabidopsis ERF012* is a versatile regulator of plant growth, development and abiotic stress responses. *International Journal of Molecular Sciences* 23:6841
20. Templalexis D, Tsitsekian D, Liu C, Daras G, Šimura J, et al. 2022. Potassium transporter TRH1/KUP4 contributes to distinct auxin-mediated root system architecture responses. *Plant Physiology* 188:1043–60
21. Wan Y, Jasik J, Wang L, Hao H, Volkmann D, et al. 2012. The signal transducer NPH3 integrates the phototropin1 photosensor with PIN2-based polar auxin transport in *Arabidopsis* root phototropism. *The Plant Cell* 24:551–65
22. Chen S, Zhou Y, Chen Y, Gu J. 2018. fastp: an ultra-fast all-in-one FASTQ preprocessor. *Bioinformatics* 34:i884–i890
23. Zhang Y, Park C, Bennett C, Thornton M, Kim D. 2021. Rapid and accurate alignment of nucleotide conversion sequencing reads with HISAT-3N. *Genome Research* 31:1290–95
24. Love MI, Huber W, Anders S. 2014. Moderated estimation of fold change and dispersion for RNA-seq data with DESeq2. *Genome Biology* 15:550
25. Varet H, Brillet-Guéguen L, Coppée JY, Dillies MA. 2016. SARTools: a DESeq2- and EdgeR-based R Pipeline for comprehensive differential analysis of RNA-Seq data. *PLoS One* 11:e0157022
26. He C, Luo C, Yan J, Zhai X, Liu W, et al. 2024. Genome-wide identification of the OVATE family proteins and functional analysis of *BhiOFP1*, *BhiOFP5*, and *BhiOFP18* during fruit development in wax gourd (*Benincasa hispida*). *Plant Physiology and Biochemistry* 216:109135
27. Chen C, Chen H, Zhang Y, Thomas HR, Frank MH, et al. 2020. TBtools: an integrative toolkit developed for interactive analyses of big biological data. *Molecular Plant* 13:1194–202
28. Ikeyama Y, Tasaka M, Fukaki H. 2010. RLF, a cytochrome b_5-like heme/steroid binding domain protein, controls lateral root formation independently of ARF7/19-mediated auxin signaling in *Arabidopsis thaliana*. *The Plant Journal* 62:865–75
29. Mangano S, Denita-Juarez SP, Choi HS, Marzol E, Hwang Y, et al. 2017. Molecular link between auxin and ROS-mediated polar growth. *Proceedings of the National Academy of Sciences of the United States of America* 114:5289–94
30. Roychoudhry S, Kepinski S. 2021. Auxin in root development. *Cold Spring Harbor Perspectives in Biology* 14:a039933
31. Rahman A, Bannigan A, Sulaman W, Pechter P, Blancaflor EB, et al. 2007. Auxin, actin and growth of the *Arabidopsis thaliana* primary root. *The Plant Journal* 50:514–28
32. Zhu J, Geisler M. 2015. Keeping it all together: auxin-actin crosstalk in plant development. *Journal of Experimental Botany* 66:4983–98
33. Bahmani R, Kim DG, Modareszadeh M, Thompson AJ, Park JH, et al. 2020. The mechanism of root growth inhibition by the endocrine disruptor bisphenol A (BPA). *Environmental Pollution* 257:113516
34. Han EH, Petrella DP, Blakeslee JJ. 2017. 'Bending' models of halotropism: incorporating protein phosphatase 2A, ABCB transporters, and auxin metabolism. *Journal of Experimental Botany* 68:3071–89
35. Barbez E, Kubeš M, Rolčík J, Béziat C, Pěnčík A, et al. 2012. A novel putative auxin carrier family regulates intracellular auxin homeostasis in plants. *Nature* 485:119–22
36. Chen J, Hu Y, Hao P, Tsering T, Xia J, et al. 2023. ABCB-mediated shootward auxin transport feeds into the root clock. *Embo Reports* 24:e56271
37. Peer WA, Blakeslee JJ, Yang H, Murphy AS. 2011. Seven things we think we know about auxin transport. *Molecular Plant* 4:487–504
38. Swarup K, Benková E, Swarup R, Casimiro I, Péret B, et al. 2008. The auxin influx carrier LAX3 promotes lateral root emergence. *Nature Cell Biology* 10:946–54
39. González-Hernández AI, Scalschi L, García-Agustín P, Camañes G. 2020. Exogenous carbon compounds modulate tomato root development. *Plants* 9:387
40. Péret B, Middleton AM, French AP, Larrieu A, Bishopp A, et al. 2013. Sequential induction of auxin efflux and influx carriers regulates lateral root emergence. *Molecular Systems Biology* 9:699
41. Zhu H, Li H, Yu J, Zhao H, Zhang K, et al. 2023. Regulatory Mechanisms of *ArAux/IAA13* and *ArAux/IAA16* in the Rooting Process of *Acer rubrum*. *Genes* 14:1206
42. Wang W, Zheng Y, Qiu L, Yang D, Zhao Z, et al. 2024. Genome-wide identification of the *SAUR* gene family and screening for *SmSAURs* involved in root development in *Salvia miltiorrhiza*. *Plant Cell Reports* 43:165
43. Cheng B, Zhou M, Tang T, Hassan MJ, Zhou J, et al. 2023. A *Trifolium repens flavodoxin-like quinone reductase 1* (*TrFQR1*) improves plant adaptability to high temperature associated with oxidative homeostasis and lipids remodeling. *The Plant Journal* 115:369–85
44. Wang Y, Li HL, Zhou YK, Guo D, Zhu JH, et al. 2021. Transcriptomes analysis reveals novel insight into the molecular mechanisms of somatic embryogenesis in *Hevea brasiliensis*. *BMC Genomics* 22:183
45. Ajadi AA, Tong X, Wang H, Zhao J, Tang L, et al. 2020. Cyclin-dependent kinase inhibitors KRP1 and KRP2 are involved in grain filling and seed germination in rice (*Oryza sativa* L.). *International Journal of Molecular Sciences* 21:245

Copyright: © 2025 by the author(s). Published by Maximum Academic Press, Fayetteville, GA. This article is an open access article distributed under Creative Commons Attribution License (CC BY 4.0), visit https://creativecommons.org/licenses/by/4.0/.